

Heterogeneous catalysis modelling and numerical simulation in rarefied gas flows. Part I: Coverage locally at equilibrium

Isabelle Choquet

ITWM, Institut für Techno- und Wirtschaftsmathematik, Erwin-Schrodinger-Str., 67663 Kaiserslautern, Germany

*ONERA, 29 av. de la Division Leclerc, 92322 Châtillon, France **

A new approach is proposed to model and simulate numerically heterogeneous catalysis in rarefied gas flows. It is developed to satisfy all together the following points: *i)* describe the gas phase at the microscopic scale, as required in rarefied flows, *ii)* describe the wall at the macroscopic scale, to avoid prohibitive computational costs and consider not only crystalline but also amorphous surfaces, *iii)* reproduce on average macroscopic laws correlated with experimental results and *iv)* derive analytic models in a systematic and exact way.

The problem is stated in the general framework of a non static flow in the vicinity of a catalytic and non porous surface (without ageing). It is shown that the exact and systematic resolution method based on the Laplace transform, introduced previously by the author to model collisions in the gas phase, can be extended to the present problem. The proposed approach is applied to the modelling of the Eley-Rideal and Langmuir-Hinshelwood recombinations, assuming that the coverage is locally at equilibrium. The models are developed considering one atomic species and extended to the general case of several atomic species. Numerical calculations show that the models derived in this way reproduce with accuracy behaviours observed experimentally.

I. INTRODUCTION

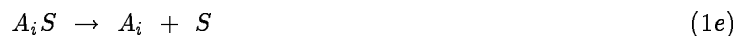
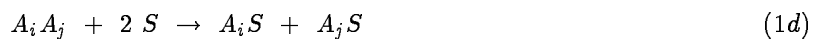
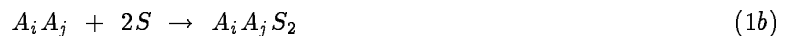
Heterogeneous catalysis affects the gas composition as well as the surfacic heat fluxes of gas flows in chemical nonequilibrium in the vicinity of surfaces, in order to tend towards chemical equilibrium. As an illustration, the additional heat flux due to catalytic recombination at the wall of a vehicle can reach up to 30% during an atmospheric reentry. Chemistry at the gas-wall interface is involved not only in hypersonic flow problems¹ but also in many industrial processes^{2,3} such as chemical reactors or laser nozzles. However, in spite of its strong influence on heat fluxes, heterogeneous catalysis has been little treated up to now in the particular framework of rarefied gas flows.⁴⁻⁹

The catalytic effect of a surface generally expresses itself through a reduction in the energy of activation of chemical reactions and an increase in transitions from unstable precursor of the molecule to stabilized molecule. Indeed, the energy released to stabilize the molecule can be given to the surface while in the gas phase an additional collision should still take place, during the short life time of the unstable precursor, to release this energy in excess.

* *Permanent address*

The necessary precursor stage of heterogeneous catalysis^{3,10-13} is the capture of gas particles by the wells of the surfacic potential. A given surface can have various types of adsorption sites of chemisorption and/or physisorption. The difference between these two kinds of adsorptions lies in the nature of the physical forces linking a gas atom to the surface. Generally, the energy of chemisorption is an order of magnitude higher than the energy of physisorption. Physisorption can thus be a precursor stage for chemisorption but not for chemical reactions, by contrast with chemisorption. The number of adsorption sites, as well as their nature, depends on the chemical composition and structure of the wall.

Adsorption applies to gas atoms, as well as gas molecules, which translational energy is not sufficient to cross the surfacic potential and go back to the gas phase. A gas atom A_i (or A_j) can then be adsorbed by a free surfacic site, S (or well of the surfacic potential), to form an adatom, A_iS (or A_jS) according to Eq. (1a).



In very rare cases molecules can be adsorbed without dissociation, Eq. (1b). This adsorption is restricted to the particular case of an interatomic distance (of the gas molecule) similar to the distance between adjacent sites. Most of the time, molecules are adsorbed with dissociation. Then, within the frame of diatomic molecules, the two atoms, Eq. (1d), or only one, Eq. (1c), are adsorbed and the other one is reflected in the gas. Adsorbed particles can form one or several layers, depending on the surface and gas composition. They can also be fixed, or move over the surface, according to the surface composition and temperature.

Adsorbed particles can be desorbed, Eqs. (1e-f), due to the thermal motion of the wall atoms. This desorption, corresponding to the reverse processes of Eqs. (1a-b), is activated when the wall atoms can give to the adsorbed particles a thermal energy sufficiently high to break the link with the surface and also to cross the surfacic potential.

Adatoms adsorbed through chemisorption can also undergo recombinations which are generally described by the Eley-Rideal (ER) and the Langmuir-Hinshelwood (LH) mechanisms. The ER recombination, Eq. (1g), involves a first reactant coming directly from the gas phase, A_i , and a second one, A_j , adsorbed at the gas-wall interface. Concerning the LH recombination, Eq. (1h), both reactants are adatoms. The molecule A_iA_j ,

obtained through ER or LH mechanism, is desorbed and emitted in the gas and one or two surfacic sites S are released. These two recombination processes can be concomitant. However, the ER recombination seems to be predominant at low surfacic temperature, when the fraction of adsorbed particles is high, while the LH recombination is predominant at higher surfacic temperature, when adsorbed particles can move over the surface.

This set of elementary processes, Eqs. (1a-h), is often characterized by two global parameters, which are strongly coupled, and that will be useful in what follows: the coverage, θ , or fraction of occupied surfacic sites, and the reaction coefficient, γ , or fraction of recombined atoms per gas atom colliding with the surface. The coverage, and more often the reaction coefficient, are the quantities experimentally measured to determine the catalytic activity of surfaces.

A first approach used to model gas-wall interaction is molecular: gas and surface are both described at the molecular scale. This approach assumes that atoms constituting the surface are regularly arranged in a periodic lattice. It is thus applied to crystalline surfaces, such as metals slowly cooled which are used to coat wind tunnel testing models for instance. It includes molecular dynamics^{14,15} and bond order conservation methods.¹⁶ The latter assumes a rigid surfacic lattice, which leads to lower numerical costs compared with the former.

A second approach of heterogeneous catalysis modelling is macroscopic: gas and surface are both described at the macroscopic scale. This approach is widely applied to continuous flows. Models are then obtained doing kinetic or statistical or thermodynamic derivations. They involve parameters determined by correlation with experimental results. At first, macroscopic models have been developed assuming a coverage at equilibrium, that is to say adsorption processes faster than recombination reactions. These models give the global change of gas composition in the vicinity of the surface, defining the coverage and recombination coefficients for the ER and LH reactions.³ A higher level of modelling has been handled more recently¹⁷⁻²¹ to study reentry flows. As required for such flows, it is no longer assumed that the coverage is at equilibrium. Forward and reverse reactions are then clearly distinguished and the reaction rates associated with each elementary process are determined.

There is still few published studies⁴⁻⁹ about heterogeneous catalysis in rarefied flows. They can also be divided into the two sets of approaches mentioned above. The macroscopic approach, although applied to rarefied flows, is investigated Refs. [4-5] by Bergemann for instance. This author describes the ER recombination and dissociation of oxygen and nitrogen on amorphous surfaces (Reaction Cured Glass or RCG, used to coat the protective tiles of reentry vehicles) assuming a coverage locally at equilibrium. His model is expressed as a function of the gas temperature and not of microscopic variables. It is thus used numerically when the macroscopic variables can be calculated (i.e. after the transient regime).

The molecular approach is treated Refs. [8-9] by Simons for instance, using the bond order conservation method. His study applies to crystalline surfaces (not to amorphous surfaces) and assumes a coverage close to unity. It is mainly focussed on the improvement of adsorption modelling with an energy of adsorption

which depends on the coverage, by contrast with the model proposed Refs. [4-5].

As heterogeneous catalysis should apply to crystalline as well as amorphous surfaces, and rarefied gas flows should be modelled at the microscopic scale, another approach is proposed here to satisfy all together the following points:

- i) describe the gas phase at the microscopic scale, as required in rarefied flows,
- ii) describe the wall at the macroscopic scale, to avoid prohibitive computational costs and consider not only crystalline but also amorphous surfaces,
- iii) reproduce on average macroscopic laws correlated with experimental results and
- iv) derive the models in a systematic and exact way, and express them under analytic form.

To that purpose, the problem is stated Sec. II in the general framework of a non static flow in the vicinity of a catalytic surface. The wall is supposed to be non porous. Moreover, it is assumed that the structure of the surface is not modified by the chemical reactions: there is no ageing or ablation of the surface since the wall atoms are not involved in the final products of the chemical reactions.

A systematic and exact resolution method of this problem, which is based on the Laplace transform, is proposed Sec. III. This resolution method has been previously introduced by the author to model rotational²² and vibrational²³ nonequilibria in the gas phase. It has been also extended to the modelling of chemistry²⁴ in the gas phase (see also Ref. [25]).

This new approach is then applied to the modelling of the ER and LH recombinations assuming, in this first part, a coverage locally at equilibrium. The demonstrations are detailed within the frame of one atomic species. The models are then extended to the general case of gas flows including several atomic species.

Numerical applications are proposed to check that these models reproduce with accuracy behaviours observed experimentally.

II. STATEMENT OF THE PROBLEM

The problem proposed below is stated to define the microscopic probabilities, denoted by p , for the various elementary processes described Eqs. (1a-h) to take place. To fulfill the conditions *i*) and *ii*) precised Sec. I, these probabilities are expressed as functions of microscopic and macroscopic variables concerning respectively the gas phase and the wall contributions. To satisfy the condition *iii*), the microscopic probabilities p are defined to reproduce on average, through $\langle p \rangle$, laws correlated with experimental results. Let us underline that the average procedure applies only to the gas phase contribution. This is the reason why one will indicate explicitly, using square brackets, the functional dependance of the microscopic and macroscopic probabilities, p and $\langle p \rangle$, with regards to the average procedure and neglect to indicate the functional dependance concerning the wall contribution for instance.

The problem is stated within the general framework of a non static flow, assuming that the surface is not porous. Its statement consists in linking the microscopic probabilities to be derived, p , to the macroscopic probabilities to be reproduced, $\langle p \rangle$. To that purpose, let us consider again the set of elementary processes

one wants to model. One can notice that adsorption processes with or without dissociation, Eqs (1a-d), as well as the ER recombination, Eq. (1g), are all initiated by a collision between a gas particle and empty or occupied surfacic sites. The LH recombination, Eq. (1h), can also be interpreted in this way remembering that it is coupled with adsorption. The macroscopic probability associated with one of these elementary processes is thus the flux of gas particles impinging on the surface that undergo the process under consideration, with the probability p , divided by the total flux of particles colliding with the surface

$$\langle p \rangle [T] = \frac{\int \int \int_{\vec{v} \cdot \vec{n} \geq 0} p \vec{v} \cdot \vec{n} f[\vec{v} - \vec{v}_o, T] d\vec{v}}{\int \int \int_{\vec{v} \cdot \vec{n} \geq 0} \vec{v} \cdot \vec{n} f[\vec{v} - \vec{v}_o, T] d\vec{v}} \quad (2a)$$

where \vec{v} is the gas particle velocity, \vec{v}_o the mean molecular velocity, \vec{n} the normalized surfacic vector, T the gas temperature. The integrals involved in Eq. (2a) are calculated over the half space $\vec{v} \cdot \vec{n} \geq 0$, since the surface is not porous. The thermal velocity distribution function of the gas particles, f , is given by a Maxwellian since the macroscopic laws to be reproduced are defined in the literature assuming equilibrium

$$f[\vec{v} - \vec{v}_o, T] = \left(\frac{m}{2\pi kT} \right)^{3/2} \exp \left[- \frac{m(\vec{v} - \vec{v}_o)^2}{2kT} \right] \quad (2b)$$

where m is the mass of a gas particle and k the Boltzmann's constant.

This statement of the problem is valid for all the elementary processes except desorption defined Eqs. (1e-f). Indeed, these desorptions are only initiated by the surface, cf. Sec. I. Opting for a macroscopic description of the surface, the probability of desorption per unit time and surface should be directly inferred from a macroscopic rate of desorption correlated with experimental results, cf. Part 2. However, the problem defined Eqs. (2a-b) has still to be solved.

III. RESOLUTION OF THE PROBLEM

To simplify the notations without restricting the problem, let us consider cartesian coordinates with the molecular velocity $\vec{v} = (v_x, v_y, v_z)$, the mean molecular velocity $\vec{v}_o = (v_{ox}, v_{oy}, v_{oz})$ and a surface perpendicular to the z axis, thus $\vec{v} \cdot \vec{n} = v_z$. The z component of the mean molecular velocity, v_{oz} , is set equal to zero since the surface is not porous. Slip effects can be taken into account with $v_{ox} \neq 0$ and/or $v_{oy} \neq 0$.

Besides, one should choose a microscopic variable associated with the impinging gas particle to express p . It is generally assumed that the energy of activation of catalytic elementary processes is given by the velocity component of the gas particle which is normal to the surface. Consequently, the individual probabilities to be defined, p , are expressed as functions of v_z . Taking into account these notations and assumptions, the problem defined Eqs. (2a-b) can write

$$\langle p \rangle [T] = \frac{\int_0^\infty v_z p[v_z] f[v_z, T] dv_z}{\int_0^\infty v_z f[v_z, T] dv_z} \quad (3a)$$

where

$$f[v_z, T] = \left(\frac{m}{2\pi kT} \right)^{1/2} \exp \left[- \frac{mv_z^2}{2kT} \right] \quad (3b)$$

The unknown p should then be derived from this integral equation assuming that the macroscopic probability, $\langle p \rangle$, is given. To obtain a systematic and exact derivation, it is shown below that the resolution method based on the Laplace transform, introduced previously by the author to model thermal nonequilibria in the gas phase,²²⁻²³ can be extended to the present problem. Indeed, doing the following changes of variables:

$$\epsilon = m (2kT)^{-1} \quad \text{and} \quad \phi = v_z^2, \quad (4a)$$

the problem formulated Eqs. (3a-b) yields

$$\epsilon^{-1} \langle p \rangle \left[\frac{m}{2k\epsilon} \right] = \int_0^\infty p[\phi^{1/2}] \exp[-\phi \epsilon] d\phi \quad (4b)$$

which is identified with

$$p[\phi^{1/2}] = \mathcal{L}^{-1} \left\{ \epsilon^{-1} \langle p \rangle \left[\frac{m}{2k\epsilon} \right] \right\} \quad (5)$$

where \mathcal{L}^{-1} denotes the inverse Laplace transform. Consequently, individual probabilities of adsorption, dissociation and recombination at the gas-wall interface, p , can be defined in a systematic and exact way deriving the inverse Laplace transform of the function $\epsilon^{-1} \langle p \rangle$, where $\langle p \rangle$ can be correlated with experimental results.

IV. APPLICATION TO A COVERAGE AT EQUILIBRIUM

To treat progressively the difficulties, it is assumed in this first part that recombination processes are slow compared with adsorption. Consequently it is not necessary to consider both adsorption and desorption processes since the coverage is supposed to be locally at equilibrium.

Several models of coverage can be found in literature¹⁰ such as Langmuir's, Freundlich's and Temkin's isotherms. These macroscopic models are developed assuming that the coverage is monolayer : adsorption is localized, it takes place only through collision of particles with vacant sites and there is no more than one adsorbed atom per site. The differences between these models lie in the energy of an adsorbed particle. While Langmuir's model assumes that the energy of adsorption is the same at any site of the surface, independently of the presence or absence of nearby adsorbed particles, Freundlich's and Temkin's models assume that it decreases with the coverage. This last behaviour could be interpreted as a surface heterogeneity or as an increasing surface repulsion with an increasing coverage. For the former the fall with the coverage is linear and for the latter it is logarithmic. Others models take into account the formation of different types of adsorbed layers. Although Freundlich's and Temkin's isotherms seem to be more realistic, we are going to consider Langmuir's isotherm. This choice is simply dictated by the available parameters, cf. Refs. [26-27] for instance, derived from experimental data.

Langmuir's isotherm is obtained from kinetic derivations, for one atomic species,

$$\theta = \frac{[n] K^{ad}}{1 + [n] K^{ad}} \quad (6a)$$

where $[n]$ is the numerical density of the gas particles subject to adsorption which are in the vicinity of the surface. The equilibrium constant of the adsorption and desorption reactions, K^{ad} , is given by an Arrhenius law

$$K^{ad} = C^{ad} \exp[+D^{ad}/(kT_w)], \quad \text{with } D^{ad} > 0 \quad (6b)$$

where C^{ad} and D^{ad} are constants depending on both the gas and the wall compositions and T_w is the wall temperature.

In the general framework of N chemical species which are in competition to occupy surfacic sites, one easily derive, under the same assumptions, the coverage associated with the chemical species j

$$\theta_j = \frac{[n_j] K_j^{ad}}{1 + \sum_{k=1}^N [n_k] K_k^{ad}} \quad (6c)$$

where $[n_k]$ and $K_k^{ad} = C_k^{ad} \exp[+D_k^{ad}/(kT_w)]$, with $D_k^{ad} > 0$, are respectively the numerical density of the gas particles in the vicinity of the surface and the equilibrium constant of the adsorption and desorption reactions, associated with the chemical species k .

The determination of the numerical density of the gas particles in the vicinity of the surface, $[n]$ or $[n_k]$, raises a difficulty: the definition of the vicinity, that is to say of the gas volume one should consider in numerical applications. Within the frame of the assumptions precised Sec. II, the numerical density $[n]$ (or $[n_k]$) can be expressed as a function of both the rate of particles-wall collisions, $[\dot{n}]$ (or $[\dot{n}_k]$) and the gas temperature

$$[n] = \sqrt{\frac{2\pi m}{kT}} [\dot{n}] \quad (6d)$$

The determination of the number of gas particles colliding with the wall per unit time and surface, $[\dot{n}]$ or $[\dot{n}_k]$, raises none difficulty. This is the reason why this rate is retained in what follows as a variable of the problem rather than the numerical density of the gas particles in the vicinity of the surface.

In this first part one starts from the ER and LH macroscopic models of chemistry at the gas-wall interface. These models assume that dissociation reactions, Eqs. (1c-d), are negligible compared with recombination reactions, Eqs. (1g) and (1h), (which corresponds with an impinging gas flow strongly dissociated). They provide the global change of gas composition in the vicinity of the surface defining the recombination coefficients, γ , for both ER and LH mechanisms. Referring to the definition of γ , which is recalled in Sec. I, it follows immediatly that the macroscopic probability to be reproduced is the recombination coefficient

$$\langle p \rangle = \gamma \quad (7)$$

A.1. Eley-Rideal recombination: particular case of one atomic species

To lighten the notations, let us first consider a gas flow made of one atomic species and the related diatomic molecules. The ER recombination coefficient³ is the fraction of gas atoms colliding with the surface that recombine with adsorbed atoms, according to the mechanism described Eq. (1g),

$$\gamma^{BR} = 2 \left(\frac{2\pi m}{kT} \right)^{1/2} k_r^{BR} \theta \quad (8a)$$

where the ER recombination reaction rate, k_r^{BR} , is given by an Arrhenius law

$$k_r^{BR} = C_r^{BR} \exp[-E_r^{BR}/(kT)], \quad \text{with } E_r^{BR} > 0 \quad (8b)$$

and C_r^{BR} and E_r^{BR} are constants depending on both the gas and the wall compositions. One can notice that for low surfacic temperature, T_w , that is to say predominant adsorption compared with desorption, the asymptotic behaviour of γ^{BR} is independent of the gas pressure, or $[\dot{n}]$. For high surfacic temperature, and thus predominant desorption, the asymptotic behaviour of γ^{BR} is proportional to $[\dot{n}]$.

The ER recombination coefficient associated with the recombination of oxygen on RCG surfaces is plotted Fig. 1, assuming a thermal equilibrium between the gas and the surface, i.e. $T = T_w$ and various atomic pressures. The experimental values^{3,28-31} plotted Fig. 1, and given Table 1, have been used by Willey^{26,27} to determine the parameters C^{ad} , D^{ad} , C_r^{BR} and E_r^{BR} which are grouped together Table 2 and used for this example.

The microscopic probability we propose is thus the probability for a gas particule colliding with a surface to collide with an occupied site and recombine. It is derived from the inverse Laplace transform, defined Eq. (5), and the macroscopic data of Eqs. (6a-b) and (6d-8b)

$$p_r^{BR}[v_z] = 4 \pi^{1/2} C_r^{BR} H[v_z^2 > 2E_r^{BR}/m] \left\{ \frac{1}{[\pi (v_z^2 - 2E_r^{BR}/m)]^{1/2}} - \alpha \exp\left[\alpha^2 (v_z^2 - 2E_r^{BR}/m)\right] \text{Erfc}\left[\alpha (v_z^2 - 2E_r^{BR}/m)^{1/2}\right] \right\} \quad (9a)$$

with

$$\alpha = \exp[-D^{ad}/(kT_w)] (2 \pi^{1/2} [\dot{n}] C^{ad})^{-1} \quad (9b)$$

where H is the Heaviside function³² and Erfc the complementary Error function.³² Let us recall that rigorously, cf. Sec. II, one should write $p_r^{BR}[v_z, [\dot{n}], T_w]$ instead of $p_r^{BR}[v_z]$.

Demonstration

The macroscopic probability to be reproduced is derived from Eqs. (6a-b) and (6d-8b) and can be expressed by

$$\langle p_r^{BR} \rangle [T] = 2 C_r^{BR} \sqrt{\frac{2\pi m}{kT}} \exp[-E_r^{BR}/(kT)] \frac{1}{1 + \alpha(2kT/m)^{1/2}} \quad (10)$$

where α is defined Eq. (9b). Taking into account the first change of variable defined Eq. (4a), and replacing $\langle p \rangle$ by Eq. (10) in Eq. (5) one can obtain

$$p_r^{BR}[\phi^{1/2}] = \mathcal{L}^{-1} \left\{ 4 \pi^{1/2} C_r^{BR} \exp[-2E_r^{BR} \epsilon/m] \frac{1}{\alpha + \epsilon^{1/2}} \right\} \quad (11)$$

Due to a similarity property of the Laplace transform,³³ Eq. (11) writes immediatly

$$p_r^{BR}[\phi^{1/2}] = 4 \pi^{1/2} C_r^{BR} \mathcal{L}^{-1} \left\{ \exp[-2E_r^{BR} \epsilon/m] \frac{1}{\alpha + \epsilon^{1/2}} \right\} \quad (12)$$

Next, showing that³³

$$\mathcal{L}^{-1} \left\{ \frac{1}{a} \exp[-b \epsilon/a] G[\epsilon/a] \right\} = H[\phi > b/a] g[a\phi - b] \quad (13)$$

with $a, b > 0$, $g[\phi] = \mathcal{L}^{-1}\{G[\epsilon]\}$, and where H denotes the Heaviside function, one can obtain

$$p_r^{BR}[\phi^{1/2}] = 4 \pi^{1/2} C_r^{BR} H[\phi > 2E_r^{BR}/m] \mathcal{L}^{-1} \left\{ \frac{1}{\alpha + \epsilon^{1/2}} \right\} [\phi - 2E_r^{BR}/m] \quad (14)$$

where the last square brackets of Eq. (14) underline that the inverse Laplace transform depends now on $\phi - 2E_r^{BR}/m$, and no longer on ϕ . Finally, showing that³³

$$\mathcal{L}^{-1} \left\{ \frac{1}{a + \epsilon^{1/2}} \right\} = (\pi \phi)^{-1/2} - a \exp[a^2 \phi] \operatorname{Erfc}[a \phi^{1/2}] \quad (15)$$

with $a > 0$ since $\epsilon > 0$, and where Erfc denotes the complementary Error function,³² Eq. (14) leads to

$$p_r^{BR}[\phi^{1/2}] = 4 \pi^{1/2} C_r^{BR} H[\phi > 2E_r^{BR}/m] \left\{ \frac{1}{[\pi (\phi - 2E_r^{BR}/m)]^{1/2}} - \alpha \exp\left[\alpha^2 (\phi - 2E_r^{BR}/m)\right] \operatorname{Erfc}\left[\alpha (\phi - 2E_r^{BR}/m)^{1/2}\right] \right\} \quad (16)$$

The individual probability given Eq. (9a) is then derived from Eq. (16) doing the second change of variable defined Eq. (4a).

A.2. Eley-Rideal recombination: general case of several atomic species

Most of the time gas flows are made of several atomic species. Various of them are then in competition to occupy surfacic sites and recombination can lead to the formation of heteronuclear molecules. In that general case the recombination coefficient, Eq. (8a), associated now with an impinging gas atom and an adsorbed atom belonging respectively to the chemical species i and j , gets

$$\gamma_{ij}^{BR} = (1 + \delta_{ij}) \left(\frac{2\pi m_i}{kT} \right)^{1/2} k_{r,ij}^{BR} \theta_j \quad (17a)$$

with the ER recombination rate

$$k_{r,ij}^{BR} = C_{r,ij}^{BR} \exp\left[-E_{r,ij}^{BR}/(kT)\right], \quad \text{with } E_{r,ij}^{BR} > 0 \quad (17b)$$

and the coverage θ_j defined Eq. (6c). δ_{ij} represents the Kronecker's symbol. Taking into account Eq. (6d) and grouping together the terms in a different way, this coverage can also write

$$\theta_j = \theta_{ij} = \frac{\beta_j}{1 + \alpha_{ij} (2kT/m_i)^{1/2}} \quad (17c)$$

where

$$\alpha_{ij} = \beta_j \left(2 \pi^{1/2} [\dot{n}_j] C_j^{ad} \sqrt{\frac{m_j}{m_i}} \right)^{-1} \exp[-D_j^{ad}/(kT_w)] \quad (17d)$$

and

$$\beta_j = \left(\sum_{k=1}^N \frac{[\dot{n}_k]}{[\dot{n}_j]} \sqrt{\frac{m_k}{m_j}} \frac{K_k^{ad}}{K_j^{ad}} \right)^{-1} \quad (17e)$$

do not depend on the gas temperature T . The macroscopic probability to reproduce expresses thus

$$\langle p_{r,ij}^{BR} \rangle [T] = (1 + \delta_{ij}) C_{r,ij}^{BR} \sqrt{\frac{2\pi m_i}{kT}} \exp[-E_{r,ij}^{BR}/(kT)] \frac{\beta_j}{1 + \alpha_{ij} (2kT/m_i)^{1/2}} \quad (18)$$

A derivation similar to that detailed above, in the particular case of only one atomic species, leads to the microscopic probability associated with the ER recombination within the general frame of several atomic species

$$p_{r,ij}^{BR}[v_z] = 2 \pi^{1/2} (1 + \delta_{ij}) \beta_j C_{r,ij}^{BR} H[v_z^2 > 2E_{r,ij}^{BR}/m_i] \left\{ \frac{1}{[\pi (v_z^2 - 2E_{r,ij}^{BR}/m_i)]^{1/2}} - \alpha_{ij} \exp\left[\alpha_{ij}^2 (v_z^2 - 2E_{r,ij}^{BR}/m_i)\right] \text{Erfc}\left[\alpha_{ij} (v_z^2 - 2E_{r,ij}^{BR}/m_i)^{1/2}\right] \right\} \quad (19)$$

where the impinging gas atom, of velocity v_z , belongs to the chemical species i and $p_{r,ij}^{BR}[v_z]$ should rigorously write $p_{r,ij}^{BR}[v_z, [\dot{n}_1], \dots, [\dot{n}_i], [\dot{n}_j], \dots, [\dot{n}_N], T_w]$.

One can easily see that, as expected, Eq. (19) reduces to Eq. (9a) in the particular case of one atomic species, i.e. $N = 1$, since then $\beta_j = 1$ and $\alpha_{ij} = \alpha$.

Remark

One could prefer to opt for individual probabilities p_r^{BR} and $p_{r,ij}^{BR}$ expressed as functions of the numerical density of the gas atoms in the vicinity of the surface, rather than the rate of atom-wall collisions. In that perspective, the approach proposed in the present paper can lead to the following individual probabilities of ER recombination regarding respectively one and several atomic species:

$$p_r^{BR}[v_z, [n], T_w] = 4 C_r^{BR} \theta H[v_z^2 > 2E_r^{BR}/m] (v_z^2 - 2E_r^{BR}/m)^{-1/2} \quad (20a)$$

and

$$p_{r,ij}^{BR}[v_z, [n_1], \dots, [n_i], [n_j], \dots, [n_N], T_w] = 2 (1 + \delta_{ij}) C_{r,ij}^{BR} \theta_j H[v_z^2 > 2E_{r,ij}^{BR}/m_i] (v_z^2 - 2E_{r,ij}^{BR}/m_i)^{-1/2} \quad (20b)$$

where θ and θ_j are given by Eqs. (6a) and (6c). The demonstrations are similar to the previous one up to Eq. (14) but the remaining function to be inversed using the Laplace transform is simply $\epsilon^{-1/2}$. The individual probabilities, Eqs. (20a-b), are then obtained showing that $\mathcal{L}^{-1}\{\epsilon^{-a}\} = \phi^{a-1}/\Gamma[a]$ with $a > 0$, and doing the second change of variable defined Eq. (4a). Γ denotes the Gamma function.³²

B.1. Langmuir-Hinshelwood recombination: particular case of one atomic species

One consider first a gas flow made of one atomic species and the related diatomic molecules, to lighten the notations. The LH recombination coefficient³ is the fraction of atoms colliding with the surface that are first adsorbed and then recombine with another adatom encountered after migration over the surface, according to the mechanism described Eqs. (1a) and (1h) for instance,

$$\gamma^{LH} = \frac{2}{[\dot{n}]} \left(\frac{2\pi m}{kT} \right)^{1/2} k_r^{LH} \theta^2 \quad (21a)$$

where k_r^{LH} is the LH recombination reaction rate

$$k_r^{LH} = C_r^{LH} \exp[-E_r^{LH}/(kT)], \quad \text{with } E_r^{LH} > 0 \quad (21b)$$

The main difference compared with the ER mechanism lies in the squared coverage, since the impinging gas atom should now be adsorbed before recombination. One can notice that for low surfacic temperature, i.e. predominant adsorption, the asymptotic behaviour of γ^{LH} is inversely proportional to the gas pressure, or $[\dot{n}]$. For high surfacic temperature, i.e. predominant desorption, the asymptotic behaviour of γ^{LH} is proportional to $[\dot{n}]$. So, contrary to the ER recombination coefficient, the LH recombination coefficient depends, in both limiting cases, on $[\dot{n}]$.

The LH recombination coefficient associated with the recombination of oxygen on RCG surfaces is plotted Fig. 2, assuming a thermal equilibrium between the gas and the surface, i.e. $T = T_w$ and various atomic pressures. The experimental values^{3,28-31} plotted Fig. 2, and given Table 2, have been used by Willey²⁶⁻²⁷ to determine the parameters C^{ad} , D^{ad} , C_r^{LH} and E_r^{LH} which are grouped together Table 2 and used for this example.

The related LH microscopic probability we propose, or probability for a gas atom colliding with the surface to collide with an empty site, be adsorbed and recombine with another adatom, is derived from the inverse Laplace transform, defined Eq. (5), and the macroscopic data of Eqs. (6a-b), (6d-7) and (21a-b)

$$\begin{aligned} p_r^{LH}[v_z] &= \frac{4}{[\dot{n}]} C_r^{LH} H[v_z^2 > 2E_r^{LH}/m] \\ &\times \left\{ \exp[\alpha^2 (v_z^2 - 2E_r^{LH}/m)] \operatorname{Erfc}[\alpha (v_z^2 - 2E_r^{LH}/m)^{1/2}] \left[\frac{1}{2} + \alpha^2 (v_z^2 - 2E_r^{LH}/m) \right] \right. \\ &\quad \left. - \frac{\alpha}{\pi^{1/2}} (v_z^2 - 2E_r^{LH}/m)^{1/2} \right\} \end{aligned} \quad (22)$$

where H is the Heaviside function, Erfc is the complementary Error function and α is defined Eq. (9b). Rigorously, one should write $p_r^{LH}[v_z, [\dot{n}], T_w]$ instead of $p_r^{LH}[v_z]$

Demonstration

The macroscopic probability to be reproduced is derived from Eqs. (6a-b), (6d-7) and (21a-b). One can write

$$\langle p_r^{LH} \rangle [T] = \frac{2}{[\dot{n}]} C_r^{LH} \exp[-E_r^{LH}/(kT)] \frac{1}{(1 + \alpha(2kT/m)^{1/2})^2} \quad (23)$$

Taking into account the first change of variable defined Eq. (4a), and replacing $\langle p \rangle$ by Eq. (23) in Eq. (5) leads to

$$p_r^{LH}[\phi^{1/2}] = \mathcal{L}^{-1} \left\{ \frac{2}{[\dot{n}]} C_r^{LH} \exp[-2E_r^{LH} \epsilon/m] \frac{1}{\epsilon (1 + \alpha \epsilon^{-1/2})^2} \right\} \quad (24)$$

Due to a similarity property of the Laplace transform, Eq. (24) writes immediatly

$$p_r^{LH}[\phi^{1/2}] = \frac{2}{[\dot{n}]} C_r^{LH} \mathcal{L}^{-1} \left\{ \exp[-2E_r^{LH} \epsilon/m] \frac{1}{\epsilon (1 + \alpha \epsilon^{-1/2})^2} \right\} \quad (25)$$

Next, applying Eq. (13) one obtains

$$p_r^{LH}[\phi^{1/2}] = \frac{2}{[\dot{n}]} C_r^{LH} H[\phi > 2E_r^{LH}/m] \mathcal{L}^{-1} \left\{ \frac{1}{\epsilon (1 + \alpha \epsilon^{-1/2})^2} \right\} [\phi - 2E_r^{LH}/m] \quad (26)$$

Here again the last square brackets of Eq. (26) underline that the inverse Laplace transform depends now on $\phi - 2E_r^{LH}/m$, and no longer on ϕ . To derive the inverse Laplace transform involved in Eq. (26), let us set two functions G_1 and G_2

$$G_1[\epsilon] = \epsilon^{1/2} \quad (27a)$$

$$G_2[\epsilon] = \frac{1}{(1 + \alpha^{-1} \epsilon)^2} \quad (27b)$$

such that

$$\mathcal{L}^{-1} \left\{ \frac{1}{\epsilon (1 + \alpha \epsilon^{-1/2})^2} \right\} = \alpha^{-2} \mathcal{L}^{-1} \{ G_2[G_1[\epsilon]] \} \quad (27c)$$

Referring to the properties of the Laplace transform and componned functions³³ one knows that the right part of Eq. (27c) can also write

$$\mathcal{L}^{-1} \{ G_2[G_1[\epsilon]] \} = \int_0^\infty g_1[\psi, \phi] g_2[\psi] d\psi \quad (28)$$

where $g_2[\psi] = \mathcal{L}^{-1} \{ G_2[\epsilon] \}$ and $g_1[\psi, \phi] = \mathcal{L}^{-1} \{ \exp[-\psi G_1[\epsilon]] \}$. Next, showing that³³

$$\mathcal{L}^{-1} \left\{ \frac{b}{(1 + a\epsilon)^2} \right\} = \frac{b}{a^2} \psi \exp[-\psi/a] \quad (29a)$$

and

$$\mathcal{L}^{-1} \{ \exp[-\psi \epsilon^{1/2}] \} = (4 \pi \phi^3)^{-1/2} \psi \exp[-\psi^2/(4\phi)] \quad (29b)$$

Eq. (28) yields

$$\mathcal{L}^{-1} \{ G_2[G_1[\epsilon]] \} [\phi] = \frac{\alpha^2}{(4 \pi \phi^3)^{1/2}} \int_0^\infty \psi^2 \exp[-\alpha \psi] \exp[-\psi^2/(4\phi)] d\psi \quad (30)$$

One can recognize, Eq. (30), a direct Laplace transform applied to the variables $\tilde{\phi} = \psi^2$ and $\tilde{\epsilon} = 1/(4\phi)$; thus

$$\mathcal{L}^{-1} \{ G_2[G_1[\epsilon]] \} [\phi] = \frac{\alpha^2}{4 (\pi \phi^3)^{1/2}} \mathcal{L}^{+1} \{ \tilde{\phi}^{1/2} \exp[-\alpha \tilde{\phi}^{1/2}] \} [\tilde{\epsilon} = \frac{1}{4\phi}] \quad (31)$$

where \mathcal{L}^{+1} denotes the direct Laplace transform. Let us set a new function, g_3 , defined by

$$g_3[\tilde{\phi}] = \tilde{\phi}^{-1/2} \exp[-\alpha \tilde{\phi}^{1/2}] \quad (32a)$$

such that Eq. (31) can express

$$\mathcal{L}^{-1}\{G_2[G_1[\epsilon]]\}[\phi] = \frac{\alpha^2}{4(\pi\phi^3)^{1/2}} \mathcal{L}^{+1}\{\tilde{\phi} g_3[\tilde{\phi}]\}[\tilde{\epsilon} = \frac{1}{4\phi}] \quad (32b)$$

Then, referring to the derivation properties of the Laplace transform³³ one knows that

$$\mathcal{L}^{+1}\{\tilde{\phi} g_3[\tilde{\phi}]\}[\tilde{\epsilon}] = -\frac{dG_3[\tilde{\epsilon}]}{d\tilde{\epsilon}} \quad (32c)$$

where $\mathcal{L}^{+1}\{g_3[\tilde{\phi}]\}[\tilde{\epsilon}] = G_3[\tilde{\epsilon}]$. Besides, showing that³³

$$\mathcal{L}^{+1}\{(\pi\tilde{\phi})^{-1/2} \exp[-2(a\tilde{\phi})^{1/2}]\} = \tilde{\epsilon}^{-1/2} \exp[a/\tilde{\epsilon}] \operatorname{Erfc}[(a/\tilde{\epsilon})^{1/2}] \quad (33)$$

and remembering that the first order derivative of the complementary Error function,³² $\operatorname{Erfc}(x)$, is $-2\pi^{-1/2} \exp[-x^2]$, one obtains

$$\mathcal{L}^{+1}\{\tilde{\phi} g_3[\tilde{\phi}]\}[\tilde{\epsilon}] = \pi^{1/2} \tilde{\epsilon}^{-3/2} \exp[\alpha^2(4\tilde{\epsilon})^{-1}] \operatorname{Erfc}[\alpha(4\tilde{\epsilon})^{-1/2}] \left[\frac{1}{2} + \alpha^2(4\tilde{\epsilon})^{-1}\right] - \alpha(2\tilde{\epsilon}^2)^{-1} \quad (34)$$

Next, $\tilde{\epsilon}$ is replaced by $1/(4\phi)$ to derive $\mathcal{L}^{-1}\{G_2[G_1[\epsilon]]\}$, which is defined Eq. (32b), starting from Eq. (34). The individual probability of Eq. (26) is then inferred from the previous expression through Eq. (27c). Finally, the individual probability given Eq. (22) is derived from this last result doing the second change of variable defined Eq. (4a).

B.2. Langmuir-Hinshelwood recombination: general case of several atomic species

Within the general frame of various atomic species, the LH recombination coefficient, Eq. (21a), associated with an impinging gas atom of chemical species i and an adatom of chemical species j gets

$$\gamma_{ij}^{LH} = \frac{1 + \delta_{ij}}{[n_i]} \left(\frac{2\pi m_i}{kT}\right)^{1/2} k_{r,ij}^{LH} \theta_{ii} \theta_{ij} \quad (35a)$$

with the LH recombination rate

$$k_{r,ij}^{LH} = C_{r,ij}^{LH} \exp[-E_{r,ij}^{LH}/(kT)], \quad \text{with } E_{r,ij}^{LH} > 0 \quad (35b)$$

the coverages θ_{ii} and θ_{ij} defined Eq. (17c) and where δ_{ij} denotes the Kronecker's symbol. Referring to Eq. (7), the macroscopic probability to reproduce expresses thus

$$\langle P_{r,ij}^{LH} \rangle [T] = \frac{1 + \delta_{ij}}{[n_i]} C_{r,ij}^{LH} \exp[-E_{r,ij}^{LH}/(kT)] \frac{\beta_i \beta_j}{\left(1 + \alpha_{ii}(2kT/m_i)^{1/2}\right) \left(1 + \alpha_{ij}(2kT/m_i)^{1/2}\right)} \quad (36)$$

where α_{ii} , α_{ij} , β_i and β_j are defined Eqs. (17d) and (17e). A derivation similar to that detailed above leads to the microscopic probability associated with the LH recombination between adatoms belonging to the same chemical species i

$$\begin{aligned} p_{r,ii}^{LH}[v_z] &= \frac{4}{[\dot{n}_i]} C_{r,ii}^{LH} \beta_i^2 H[v_z^2 > 2E_{r,ii}^{LH}/m_i] \\ &\times \left\{ \exp[\alpha_{ii}^2 (v_z^2 - 2E_{r,ii}^{LH}/m_i)] \operatorname{Erfc}[\alpha_{ii} (v_z^2 - 2E_{r,ii}^{LH}/m_i)^{1/2}] \left[\frac{1}{2} + \alpha_{ii}^2 (v_z^2 - 2E_{r,ii}^{LH}/m_i) \right] \right. \\ &\quad \left. - \frac{\alpha_{ii}}{\pi^{1/2}} (v_z^2 - 2E_{r,ii}^{LH}/m_i)^{1/2} \right\} \end{aligned} \quad (37a)$$

One can easily see that Eq. (37a) reduces to Eq. (22) in the particular case of one atomic species subject to adsorption, i.e. $N = 1$.

When the LH recombination involves a gas atom belonging to the chemical species i (adsorbed after collision with an empty surfacic site) and an adatom of chemical species j , with $i \neq j$, the derivation detailed below leads to the individual probability

$$\begin{aligned} p_{r,ij}^{LH}[v_z] &= \frac{1 + \delta_{ij}}{[\dot{n}_i]} C_{r,ij}^{LH} \frac{\beta_i \beta_j}{\alpha_{ij} - \alpha_{ii}} H[v_z^2 > 2E_{r,ij}^{LH}/m_i] \\ &\times \left\{ \frac{1}{2} (\alpha_{ii} - \alpha_{ij}) (v_z^2 - 2E_{r,ij}^{LH}/m_i)^{-1/2} \right. \\ &\quad - \alpha_{ii} \exp[\alpha_{ii}^2 (v_z^2 - 2E_{r,ij}^{LH}/m_i)] \operatorname{Erfc}[\alpha_{ii} (v_z^2 - 2E_{r,ij}^{LH}/m_i)^{1/2}] \\ &\quad \left. + \alpha_{ij} \exp[\alpha_{ij}^2 (v_z^2 - 2E_{r,ij}^{LH}/m_i)] \operatorname{Erfc}[\alpha_{ij} (v_z^2 - 2E_{r,ij}^{LH}/m_i)^{1/2}] \right\} \end{aligned} \quad (37b)$$

The particular case $i = j$ can be inferred from Eq. (37b) passing to the limit α_{ij} to α_{ii} . Again, a rigorous writing would be $p_{r,ij}^{LH}[v_z, [\dot{n}_1], \dots, [\dot{n}_i], [\dot{n}_j], \dots, [\dot{n}_N], T_w]$ instead of $p_{r,ij}^{LH}[v_z]$.

Demonstration

When several atomic species are in competition to occupy surfacic sites and the LH recombination involves adatoms belonging to different chemical species, the demonstration is similar to the previous one up to the definition of the function G_1 , Eq. (27a). Next, one should set a new function

$$\tilde{G}_2[\epsilon] = \frac{1}{(1 + \alpha_{ii}^{-1} \epsilon) (1 + \alpha_{ij}^{-1} \epsilon)} \quad (38a)$$

such that

$$p_{r,ij}^{LH}[\phi^{1/2}] = \frac{1 + \delta_{ij}}{[\dot{n}_i]} C_{r,ij}^{LH} \beta_i \beta_j H[\phi > 2E_{r,ij}^{LH}/m_i] \mathcal{L}^{-1} \left\{ \alpha_{ii}^{-1} \alpha_{ij}^{-1} \tilde{G}_2[G_1[\epsilon]] \right\} [\phi - 2E_{r,ij}^{LH}/m_i] \quad (38b)$$

Referring to Eqs. (28) and (29b) and showing that³³

$$\mathcal{L}^{-1} \left\{ \frac{1}{(1 + a \epsilon) (1 + b \epsilon)} \right\} = \frac{\exp[-\psi/a] - \exp[-\psi/b]}{a - b}, \quad \text{with } a \neq b \quad (39)$$

yields to

$$\mathcal{L}^{-1} \left\{ \tilde{G}_2[G_1[\epsilon]] \right\} [\phi] = \frac{\alpha_{ii} \alpha_{ij}}{(\alpha_{ij} - \alpha_{ii}) (4 \pi \phi^3)^{1/2}} \int_0^\infty \psi (\exp[-\alpha_{ii} \psi] - \exp[-\alpha_{ij} \psi]) \exp[-\psi^2/(4\phi)] d\psi \quad (40)$$

One can recognize, Eq. (40), a direct Laplace transform applied to the variables $\tilde{\phi} = \psi^2$ and $\tilde{\epsilon} = 1/(4\phi)$; thus

$$\mathcal{L}^{-1}\left\{\tilde{G}_2[G_1[\epsilon]]\right\}[\phi] = \frac{\alpha_{ii} \alpha_{ij}}{(\alpha_{ii} - \alpha_{ij}) 4 (\pi \phi^3)^{1/2}} \mathcal{L}^{+1}\left\{\exp[-\alpha_{ii} \tilde{\phi}^{1/2}] - \exp[-\alpha_{ij} \tilde{\phi}^{1/2}]\right\}[\tilde{\epsilon} = \frac{1}{4\phi}] \quad (41)$$

This direct Laplace transform can be easily derived showing that³³

$$\mathcal{L}^{+1}\left\{\exp[-2(a \tilde{\phi})^{1/2}]\right\} = (a \pi)^{1/2} \left[\tilde{\epsilon}^{-1} - \tilde{\epsilon}^{-3/2} \exp[a/\tilde{\epsilon}] \operatorname{Erfc}[(a/\tilde{\epsilon})^{1/2}] \right] \quad (42)$$

Next Eq. (38b) is expressed using this last result and Eq. (37b) is finally obtained doing the second change of variable defined Eq. (4a).

Remark

Here again one could prefer to opt for individual probabilities p_r^{LH} and $p_{r,ij}^{LH}$ expressed as functions of the numerical density of the gas atoms in the vicinity of the surface, instead of the rate of atom-wall collisions, to obtain

$$p_r^{LH}[v_z, [n], T_w] = \frac{4}{[n]} C_r^{LH} \theta^2 H[v_z^2 > 2E_r^{LH}/m] (v_z^2 - 2E_r^{LH}/m)^{-1/2} \quad (43a)$$

within the frame of only one atomic specy and

$$p_{r,ij}^{LH}[v_z, [n_1], \dots, [n_i], [n_j], \dots, [n_N], T_w] = \frac{4}{[n_i]} C_{r,ij}^{LH} \theta_i \theta_j H[v_z^2 > 2E_{r,ij}^{LH}/m_i] (v_z^2 - 2E_{r,ij}^{LH}/m_i)^{-1/2} \quad (43b)$$

when several atomic species are in competition for adsorption. The coverage θ is given Eq. (6a) and θ_i and θ_j are defined Eq. (6c). One can refer to the Remark of the previous section concerning the demonstrations.

V. NUMERICAL APPLICATIONS

Heterogeneous catalysis can take place following collisions between gas particles and surfaces. Consequently its numerical simulation belongs to the trajectography phase of numerical codes, whatever numerical method one opts for (Monte Carlo³⁴ or particle³⁵⁻³⁶ for instance). It includes two stages detailed below: the selection, among the gas particles colliding with the surfaces, of the gas particles subject to elementary processes of heterogeneous catalysis, and the distribution of energy between gas and surface during these elementary processes.

A. Selection of particles subject to heterogeneous catalysis

Elementary processes of adsorption and desorption are not simulated in this first part since the coverage is assumed to be locally at equilibrium. However, the selection of gas atoms subject to heterogeneous catalysis is not restricted to the selection of gas particles colliding with surfaces that undergo an ER or LH recombination process, Eqs. (1g-h). Indeed, assuming a coverage at equilibrium, one adsorbed atom involved in the product of each recombination process should be replaced by another gas atom colliding with the surface, to satisfy the conservation laws. So, for each gas atom selected for recombination, another one

should be selected for removal. The following procedure is thus proposed. The list of gas particles colliding with the surface is prepared at each time step and for each surfacic cell. Since it is assumed, in this first part, that dissociation processes are negligible compared with recombination ones, cf. Sec. IV, molecules are simply reflected in the gas and the list can be restricted to atoms. Reflection can be specular, diffuse, or obey Cercignani-Lampis' model³⁷ for instance. When the list is complete, it is split in two parts:

i) atoms colliding with the surface which are allowed to recombine according to the ER or LH mechanisms and

ii) atoms colliding with the surface which are not allowed to recombine.

This selection obeys the recombination probability derived Eq. (9a) or (22) within the frame of a single atomic species, and Eq. (19) or (37a-b) when various chemical species are in competition for adsorption. It is done using the acceptance-rejection method.

Next, the list of atoms colliding with the surface which are not allowed to recombine is also split in two parts:

i) atoms to be removed, to replace atoms desorbed through recombination, and

ii) atoms reflected in the gas.

B. Energy distribution

The distribution of energy between a wall and the energy modes of a molecule obtained through recombination at the gas-wall interface should differ, depending on the recombination mechanism under consideration.

Indeed, the ER mechanism involves a gas particle, an adatom which is partially or fully accommodated and it leads to the formation of a molecule which is generally not fully accommodated with the surface. By contrast, the LH mechanism assumes that the two adsorbed particles can accommodate with the surface, while moving over it, and the molecule obtained after recombination is then fully accommodated with the surface. But concretely there is only very few pieces of informations concerning this splitting of energy between gas and surface³⁸⁻³⁹ and nearly none about the distribution of energy among the different energy modes of the new molecule. So, due to a lack of data, macroscopic models (such as those mentioned Sec. IV and correlated with experimental results by Willey) often include in the recombination coefficient the fraction of energy exchanged between the surface and the desorbed molecule.

To be consistent with the macroscopic models and data²⁶⁻²⁷ we start from, it is thus assumed in the present applications that the molecules formed at the gas-wall interface, through ER as well as LH mechanisms, are fully accommodated with the surface and the energy of recombination is given to the surface.

C. Numerical test

A numerical test is proposed to check that the microscopic probabilities developed Sec. IV allow to reproduce numerically, at equilibrium, the expected recombination coefficients. To that purpose, the

parameters involved in both the recombination reaction rates, C_r^{BR} , E_r^{BR} , C_r^{LH} and E_r^{LH} and the equilibrium constants of adsorption-desorption, C^{ad} and D^{ad} should be set. Let us consider for instance the parameters obtained by Willey²⁶⁻²⁷ (cf. Table 2) by correlation with the experimental results recalled Table 1, to model the recombination of oxygen on RCG surfaces. To satisfy the assumptions underlying the ER and LH models correlated with these experimental results, the gas and the surface are supposed to be in thermal equilibrium, thus $T = T_w$, and a low velocity flow is considered, $\vec{v}_o = (0.1, 0., 0.)$. The computational domain is a small rectangular box (10x10 cells) which boundaries are fluid except for a solid boundary located in $z = 0$. The gas flow is made of monoatomic and diatomic oxygen and the atomic pressure remains constant along a given calculation. Calculations are done for different values of the temperature lying within the range experimentally observed, that is to say from $1000/T = 0.5$ to 3.5 for a given atomic pressure. Various atomic pressures are also investigated: 10, 50 and 100Pa. This last value corresponds to the lower limit of the domain of pressures used by Willey.

The fractions of atoms colliding with the surface that recombine are calculated numerically using respectively the microscopic ER model, Eqs. (9a-b), and the microscopic LH model, Eqs. (9b) and (22). Their values are written out Tables 3 and 4 for each converged calculation. Comparisons between these numerical results and the macroscopic recombination coefficients one would like to reproduce are presented Figs. 3 and 4.

The excellent agreement one obtains, as function of the temperature as well as the pressure, is inherent in the proposed approach since the microscopic probabilities are developed to reproduce, on average, macroscopic models correlated with experimental results. One can notice that for low surfacic temperature the ER recombination coefficient does not vary with the pressure while the LH recombination coefficient increases with a decreasing pressure, as underlined Sec. IV.

VI. CONCLUDING REMARKS

The new approach proposed here to model heterogeneous catalysis in rarefied flows combines a microscopic description of the gas with a macroscopic description of the wall, by contrast with the previous studies which describe gas and wall at the same scale. This allows us to consider both kinds of surfaces: crystalline and amorphous and to propose analytic models directly applicable to rarefied flows.

The systematic and exact change between the microscopic and macroscopic description of the gas, at equilibrium, obtained using the Laplace transform, allows us to develop individual probabilities of catalytic recombination correlated with available experimental results, without defining and thus adjusting new parameters.

The applications, proposed in this first part, to the ER and LH recombination, reproduce numerically with accuracy the expected macroscopic data at equilibrium. They involve two assumptions rather important since the coverage is supposed to be locally at equilibrium and the energy of adsorption does not depend on the coverage. These assumptions will be reduced in the second part of this study.

ACKNOWLEDGMENTS

Prof. Dr. H. Neunzert is gratefully acknowledged for having invited the author at the Institut für Techno- und Wirtschaftsmathematik to do this work. The ONERA is also thanked for having let her resume rarefied flow problems during this stay. In addition the author wishes to thank Dr. J. Struckmeier and Dr. K. Steiner for usefull discussions, S. Antonov for his assistance with the PARBOSS code and all the ITWM team for its warm welcome.

REFERENCES

- ¹D. A. Stewart, J. V. Rakich and M. J. Lanfranco, "Catalytic Surface Effects Experiment on Space Shuttle," AIAA Paper 81-1143, Palo Alto, California, June 23-25 1981.
- ²E. J. Jumper, R. G. Wilkins and B. L. Preppernau, "Adaptation of a Wall-Catalytic Fluorine Recombination Model to Fluid-Dynamic Computations in an HF Laser Nozzle," AIAA Paper 85-1598, Cincinnati, Ohio, July 16-18 1985.
- ³R. P. H. Gasser, *An Introduction to Chemisorption and Catalysis by Metals*, Ed. Clarendon Press, Oxford, UK, 1985.
- ⁴F. Bergemann, "Gaskinetische Simulation von kontinuumsnahen Hyperschallströmungen unter Berücksichtigung von Wandkatalyse," Ph.D. Thesis, Institut für Strömungsmechanik, Göttingen, Germany, 1994.
- ⁵F. Bergemann, "A Detailed Surface Chemistry Model for the DSMC Method," *Rarefied Gas Dynamics*, Vol. 2, Ed. J. Harvey and G. Lord, Oxford University Press, UK, 1995, pp. 947-953.
- ⁶J. Matsui, M. Miyabe and Y. Matsumoto, "A Molecular Dynamics Study of Gas-Surface Interaction with Adosrbates," *Rarefied Gas Dynamics*, Vol. 2, Ed. J. Harvey and G. Lord, Oxford University Press, UK, 1995, pp. 1072-1078.
- ⁷J. Bömer and A. E. Beylich, "MD-Simulation of Inelastic Molecular Collisions with Condensed Matter Surfaces," 20th International Symposium on Rarefied Gas Dynamics, Beijing, China, 1996.
- ⁸R. S. Simmons and R.G. Lord, "DSMC Simulation of Hypersonic Metal Catalysis in a Rarefied Hypersonic Nitrogen/Oxygen Flow," 20th International Symposium on Rarefied Gas Dynamics, Beijing, China, 1996.
- ⁹R. S. Simmons, "Direct Simulation Monte Carlo Modelling of Surface Catalytic Events in High Enthalpy Rarefied Gas Flows," Ph.D. Thesis, Oxford University, UK, 1996.
- ¹⁰D. O. Hayward and B. M. W. Trapnell, *Chemisorption*, Ed. Butterworths, London, UK, 1964.
- ¹¹*The Solid-Gas Interface*, Ed. E. Alison Flood, New York, 1967.
- ¹²G. A. Somorjai, *Principles of Surface Chemistry*, Ed. Prentice Hall, Englewood Cliffs, New Jersey, 1972.
- ¹³M. W. Roberts and C. S. McKee, *Chemistry of the Metal-Gas Interface*, Ed. Clarendon Press, Oxford, UK, 1978.
- ¹⁴P. W. Atkins, *Molecular Quantum Mechanics*, Ed. Oxford University Press, UK, 1986.
- ¹⁵S. M. Levine and S. H. Garofalini, "Computer Simulation of Interactions of Model Pt Particles and Films with the Silica Surface," *Journal of Chemical Physics*, Vol. 88, No. 2, 1988.
- ¹⁶E. Shustorovitch, "The Bond Order Conservation Approach to Chemisorption and Heterogeneous Catalysis: Applications and Implications," *Advanced Catalysis*, Vol. 37, 1990.
- ¹⁷W. A. Seward, "A Model for Oxygen Atom Recombination on Silicon Dioxide Surface," Ph.D. Thesis, Air University, Ohio, 1985.

- ¹⁸E. J. Jumper, N. Newman, D. R. Kitchen and W. A. Seward, "Recombination of Nitrogen on Silica-Based, Thermal-Protection-Tile-Like Surfaces," AIAA Paper 93-0477, Reno, NV, Jan. 11-14 1993.
- ¹⁹S. Reggiani, M. Barbato, C. Bruno and J. Muylaert, "Model for Heterogeneous Catalysis on Metal Surfaces with Applications to Hypersonic Flows," AIAA Paper 96-1902, New Orleans, LA, June 17-20 1996.
- ²⁰A. Daiß, "Modellierung heterogener Reaktionen auf Siliziumdioxidoberflächen unter Berücksichtigung von Verdünnungseffekten," Ph.D. Thesis, Stuttgart University, Germany, 1996.
- ²¹A. Daiß, H. H. Frühauf and E. W. Messerschmid, "Modeling of Catalytic Reactions on Silica Surfaces with Consideration of Slip Effects," Journal of Thermophysics and Heat Transfer, Vol. 11, No. 3, July-Sept. 1997, pp. 346-352.
- ²²I. Choquet, "Thermal Nonequilibrium Modeling using the Direct Simulation Monte Carlo Method: Application to Rotational Energy", Physics of Fluids, Vol. 6, No. 12, Dec. 1994, pp. 4042-4053.
- ²³I. Choquet, "Vibrational Nonequilibrium Modeling using Direct Simulation. Part 1: Continuous Internal Energy", Journal of Thermophysics and Heat Transfer, Vol. 9, No. 3, July-September 1995, pp. 446-455.
- ²⁴I. Choquet, "Chemistry Modeling in Rarefied Flows", Rarefied Gas Dynamics, Ed. Ching Shen, Peking University Press, Beijing, China, 1997, pp. 681-686.
- ²⁵W. Sack, "Modellierung und numerische Berechnung von reaktiven Strömungen in verdünnten Gasen," Ph.D. Thesis, Kaiserslautern University, Germany, 1995.
- ²⁶R. J. Willey, "Mechanistic Model for Catalytic Recombination During Aerobraking Maneuvers, Final Report, NASA Grant NAG-9-314, Nov. 1989.
- ²⁷R. J. Willey, "Comparison of Kinetic Models for Atom Recombination on High-Temperature Reusable Surface Insulation," Journal of Thermophysics and Heat Transfer, Vol. 7, No. 1, Jan.-March 1993, pp. 55-62.
- ²⁸R. J. Willey, "Arc Jet Diagnostics Tests, Final Report", NASA-JSC/ASEE SFF, 1988.
- ²⁹W. J. Marinelli, "Collisional Quenching of Atoms and Molecules on Spacecraft Thermal Protection Surfaces", AIAA Paper 88-2667, June 1988.
- ³⁰P. Kolodziej and D. A. Stewart, "Nitrogen Recombination on High-Temperature Reusable Surface Insulation and the Analysis of its Effects on Surface Catalysis", AIAA Paper 87-1637, June 1987.
- ³¹C. D. Scott, "Catalytic Recombination of Nitrogen and Oxygen on High-Temperature Reusable Surface Insulation", Aerothermodynamic and Planetary Entry, Ed. by A. L. Crosbie, Progress in Astronautics and Aeronautics, Vol. 77, 1981, pp. 192-212.
- ³²*Handbook of Mathematical Functions, with Formulas, Graphs, and Mathematical Tables*, Ed. M. Abramowitz and I. A. Stegun, Dover Publication, New York, 1970.
- ³³J. Hadlik, *La Transformation de Laplace à Plusieurs Variables*, Ed. Masson and Cie., Paris, France, 1969.
- ³⁴G. A. Bird, *Molecular Gas Dynamics and Direct Simulation of Gas Flow*, Ed. Clarendon Press, Oxford, UK, 1994.

³⁵H. Neunzert and J. Struckmeier, "Particle Methods for the Boltzmann Equation," *Acta Numerica* 1995, Cambridge, UK, pp. 417-457.

³⁶J. Struckmeier and K. Steiner, "A Comparison of Simulation Methods for Rarefied Gas Flows," *Physics of Fluids*, Vol. 7, 1995, pp. 2876-2885.

³⁷C. Cercignani and M. Lampis, "Kinetic Models for Gas-Surface Interactions," *Transport Theory and Statistical Physics*, Vol. 1, No. 2, 1971, pp. 101-114.

³⁸G. A. Melin and R. J. Madix, "Energy Accommodation During Oxygen Atom Recombination on Metal Surfaces," *Transactions of the Faraday Society*, Vol. 67, No. 577, Jan. 1971, pp. 198-211.

³⁹B. Halpern and D. E. Rosner, "Chemical Energy Accommodation at Catalyst Surfaces," *Chemical Society London Faraday Transaction I, Physical Chemistry*, Vol. 74, 1978, pp. 1883-1912.

Table 1: Oxygen recombination on RCG surfaces: Experimental results.

Reference	T (K)	P (Pa)	γ (10^3)
Willey ²⁸	1557	241	8.37
	1552	134	27.93
	1540	252	8.85
	1527	253	10.81
	1522	127	16.37
	1518	241	8.17
	1501	237	15.34
	1497	239	8.38
	1486	230	21.48
	1479	128	19.72
	1458	225	24.32
	1456	124	11.46
1449	231	15.00	
Marinelli ²⁹	300	133	0.20
Kolodziej and Sewards ³⁰	1831	824	3.70
	1806	412	10.07
	1742	412	18.93
	1726	824	5.25
	1644	235	10.68
	1617	412	9.68
	1592	235	30.60
	1450	235	17.90
Scott ³¹	1647	370	23.61
	1493	368	13.00
	1419	351	7.75
Sewards et al. ¹	1556	451	17.33
	1344	406	11.20

Table 2: ER and LH recombination of oxygen on RCG surfaces: Willey's parameters²⁶⁻²⁷

Model	Parameter	Oxygen	Nitrogen
Eley Rideal	C^{ad} (m^3/atom)	$9.717 \cdot 10^{-40}$	$1.231 \cdot 10^{-33}$
	D^{ad} (kJ/mole)	574.3	404.2
	C_r^{ER}	8.5446	9.6464
	E_r^{ER} (kJ/mole)	15.7	15.97
Langmuir Hinshelwood	C^{ad} (m^3/atom)	$1.81 \cdot 10^{-38}$	$1.965 \cdot 10^{-19}$
	D^{ad} (kJ/mole)	574.3	574.3
	C_r^{LH} ($\text{atom}/\text{m}^2/\text{s}$)	$8.148 \cdot 10^{+22}$	$1.528 \cdot 10^{+23}$
	E_r^{LH} (kJ/mole)	12.68	14.21

Table 3: ER recombination of oxygen on RCG surfaces.

Numerical results obtained using Eqs. (9a-b).

P (Pa)	10	50	100
T (K)	$\gamma (10^3)$		
1800.00	0.20	1.15	0.26
1600.00	9.78	13.50	9.60
1333.33	12.3	12.4	12.3
1000.00	8.95	8.80	8.99
800.00	6.29	6.45	6.40
666.66	4.17	4.30	4.09
571.43	3.00	2.84	2.70
500.00	1.88	1.91	2.20
444.44	1.24	1.45	1.20
400.00	0.87	0.79	0.94
363.63	0.54	0.52	0.50
333.33	0.45	0.34	0.32
307.69	0.20	0.21	0.19

Table 4: LH recombination of oxygen on RCG surfaces.

Numerical results obtained using Eqs. (9b) and (22).

P (Pa)	10	50	100
T (K)	$\gamma (10^3)$		
1800.00	28.0	34.6	0.04
1600.00	375.	75.3	3.60
1333.33	288.	57.0	29.2
1000.00	170.	34.0	19.5
800.00	103.	21.5	10.0
666.66	66.0	13.4	6.80
571.43	43.0	8.10	4.30
500.00	26.0	5.40	2.90
444.44	17.0	3.60	1.75
400.00	10.0	2.20	1.23
363.63	7.60	1.50	0.69
333.33	4.80	0.85	0.41
307.69	3.00	0.50	0.30

FIGURE CAPTIONS

Fig. 1: Recombination of oxygen on RCG surfaces. Experimental results (Exp.) and Eley-Rideal macroscopic model (ER) associated with various atomic pressures P .

Fig. 2: Recombination of oxygen on RCG surfaces. Experimental results (Exp.) and Langmuir-Hinshelwood macroscopic model (LH) associated with various atomic pressures P .

Fig. 3: Eley-Rideal recombination of oxygen on RCG surfaces. Macroscopic model (Mac. mod.) and numerical results (Num. res.) associated with various atomic pressures P .

Fig. 4: Langmuir-Hinshelwood recombination of oxygen on RCG surfaces. Macroscopic model (Mac. mod.) and numerical results (Num. res.) associated with various atomic pressures P .